Int. J. Electrochem. Sci., 7 **(2012)** 10544 - 10561

International Journal of ELECTROCHEMICAL SCIENCE
www.electrochemsci.org

Hydrodynamic Voltammograms Profiling of Metallothionein Fragment

Ondrej Zitka[1,2], Marketa Kominkova[1], Sylvie Skalickova[1], Helena Skutkova[3], Ivo Provaznik[3], Tomas Eckschlager[4], Marie Stiborova[5], Vojtech Adam[1,2], Libuse Trnkova[1,2], Rene Kizek[1,2]*

[1] Department of Chemistry and Biochemistry, Faculty of Agronomy, Mendel University in Brno, Zemedelska 1, CZ-613 00 Brno, Czech Republic, European Union
[2] Central European Institute of Technology, Brno University of Technology, Technicka 3058/10, CZ-616 00 Brno, Czech Republic, European Union
[3] Department of Biomedical Engineering, Faculty of Electrical Engineering and Communication, Brno University of Technology, Kolejni 4, CZ-612 00 Brno, Czech Republic, European Union
[4] Department of Paediatric Haematology and Oncology, 2nd Faculty of Medicine, Charles University, and University Hospital Motol, V Uvalu 84, CZ-150 06 Prague 5, Czech Republic, European Union
[5] Department of Biochemistry, Faculty of Science, Charles University, Albertov 2030, CZ-128 40 Prague 2, Czech Republic, European Union
*E-mail: kizek@sci.muni.cz

Received: 24 August 2012 / *Accepted:* 23 September 2012 / *Published:* 1 November 2012

Metallothionein is intracellular metal binding protein. It can bind essential zinc ions and also toxic metals like cadmium. In cancer research the problem of resistance of cancer cells against anticancer drugs was described. In this study we optimized an electrochemical method for exploring the differences in electrochemical signals in dependence on amino acid sequence in metallothionein. For this purpose we selected the number of fragments based on bioinformatic processing, synthesized them and made high throughput electrochemical analysis. Designed electrochemical analysis was based on automated flow injection analysis with amperometric detector using Coulochem III. Detection was carried out by glassy carbon electrode. We measured hydrodynamic voltammograms (HDVs) for 23 selected metallothionein fragments within the potential range from 100 to 1200 mV. We estimated the maxima of oxidation by processing of cumulative HDV. The oxidation maxima were dependent on amino acid composition, whereas fragments from human isoforms and some saltwater fishes' species had the highest maxima (900 mV). On the opposite side fragments of other mammals like horse, mouse and bull had the lowest potential maxima (700 mV). This should be related with the binding capacity for metal ions.

Keywords: Metallothionein; Peptides; Flow Injection Analysis; High Throughput Analysis; Bioinformatics; Bioanalysis, Electrochemistry, Carbon Electrode; Sulfhydryl Group

1. INTRODUCTION

1.1 Metallothionein

Metallothioneins, low molecular mass protein (6-7 kDa), was firstly isolated from horse renal cortex tissue in 1957 [1]. These proteins occur in whole animal kingdom with a high degree of homology. Similar proteins are expressed in bacteria, fungi and even plants [2-10]. Detoxification of toxic metals, regulation of metabolism of some important trace metals, detoxification of reactive oxygen species, and some connection with tumour disease-related processes have been identified as roles of these proteins [11-15]. Structures of metallothioneins are simple, they are rich in cysteine and do not contain aromatic amino acids. Due to the enormous diversity of a MT group, a complex classification system has been introduced by Binz and Kägi. This system involves families, subfamilies, subgroups and isoforms. Fifteen families include Vertebrate, mollusc, crustacean, Echinodermata, diptera, nematode, ciliate, fungi-I, fungi-II, fungi-III, fungi-IV, fungi-V, fungi-VI, prokaryote, and plants. The biggest family - Vertebrate - is subdivided into eleven subfamilies including five mammalian, three avian, one of batrachian, anura and teleost subfamily. Complete MT classification is summarized in Tab. 2. The most widely studied group of MTs is probably the mammalian subfamily. Four mammalian MT isoforms (MT-1 – MT-4) are known and 13 MT-like human proteins were identified [16]. It is not surprising that there have been described more than 250 structural forms, which differ at least in one amino acid in their primary structure. Amino acid composition of the protein probably plays a very important role in the interaction with metal ions both coming from polluted environment and drugs used for treatment of various diseases [17]. Its tertiary structure is divided into alpha and beta domains, which creates the cysteine clusters. Four and three divalent metal ions can be bound into alpha and beta domains, respectively. As a total, MT can bind 7 divalent or possibly 12 monovalent metal ions [18].

1.2 Electrochemical analysis of MT peptides

Isolation, separation, detection and/or quantification of MT are not easy tasks for modern bioanalytical chemistry. Thanks to MT low molecular mass and unique primary structures, commonly used methods for detection of proteins suffer from many deficiencies including insufficient specificity and sensitivity. The most frequent methods used for detection of these proteins are indirect, based on quantification of heavy metal ions occurring in their structures or on high contents of sulfhydryl groups [2,19,20]. Electrochemistry is one of the most sensitive method used for detection of these proteins, mainly thanks to catalytic signals, which are proportional to concentrations of these proteins even at pM levels [21-28]. Besides detection of whole metallothionein, its hexapeptide was also electrochemically analysed [29,30]. In addition, there was studied the complex of metallothionein fragments with cadmium(II) ions using cathodic stripping voltammetry at hanging mercury electrode using [31]. Square wave voltammetry [32] or cyclic voltammetry [33,34] has been also applied for this purpose. In this study, we attempted to use amperometric detection at glassy carbon electrode coupled with flow injection analysis for determination of structure influence of metallothionein fragments on

the obtained current responses. We used the same method as in the case of screening of adenine derivatives [35].

2. EXPERIMENTAL PART

2.1 Computational pre-treatment

The data source was the internet proteomic database Expasy (www.expasy.org). For data processing Matlab version 7.9.0 (2009b) was used. Alignment was performed by using the conservative sections of the global multiple sequence alignment using the BLOSUM50 substitution matrix. Jukes Cantor model was used for mutual distances of sequences calculation and then BIONJ (Bio Neighbor Joining) method was applied for dendrogram construction [36]. To better assess the similarity of the sequences, distribution was weighted on the number of "characters". Data were processed using MICROSOFT EXCEL® (USA) and STATISTICA.CZ Version 8.0 (Czech Republic). Results are expressed as mean ± standard deviation (S.D.) unless noted otherwise (EXCEL®).

2.2 Chemicals

Fragments of metallothionein (FMTs) were synthesized by Clonestar (Clonestar s.r.o., Brno, Czech Republic) with FMTs purity higher than 94 %. Other chemicals were purchased from Sigma Aldrich (USA) in ACS purity unless noted otherwise. Stock standard solutions of FMTs (1 mg/ml) was prepared with ACS water (Sigma-Aldrich) and stored in dark at -20 °C. Working standard solutions were prepared daily by dilution of the stock solutions. The pH value was measured using WTW inoLab Level 3 with terminal Level 3 (Weilheim, Germany), controlled by software MultiLab Pilot (Weilheim). Deionised water underwent demineralization by reverse osmosis using the instruments Aqua Osmotic 02 (Aqua Osmotic, Tisnov, Czech Republic) and then it was subsequently purified using Millipore RG (Millipore Corp., USA, 18 MΩ) – MiliQ water.

2.3 Flow injection analysis with electrochemical detection

The instrument for flow injection analysis with electrochemical detection (FIA-ED) consisted of a solvent delivery pump operating in the range of 0.001-9.999 $ml.min^{-1}$ (Model 582 ESA Inc., Chelmsford, MA, USA), a reaction coil (1 m) and an electrochemical detector. The electrochemical detector includes one low volume flow-through analytical cell (Model 5040, ESA, USA), which is consisted of glassy carbon working electrode, hydrogen-palladium electrode as reference electrode and auxiliary electrode, and Coulochem III as a control potentiostat module. A flow rate of mobile phase was 1 $ml.min^{-1}$ as optimum for FIA bioanalysis [35,37,38]. The other conditions that were optimized are shown in the Results and Discussion section. The sample (20 µl) was injected using the autosampler (Model 542, ESA, USA). The data obtained were treated by Clarity software (Version 1.2.4, Data Apex, Czech Republic). The experiments were carried out at room temperature. A glassy

carbon electrode was polished mechanically by 0.1 μm of alumina (ESA Inc., USA) and sonicated at room temperature for 5 min using a Sonorex Digital 10 P Sonicator (Bandelin, Berlin, Germany) at 40 W [39-41].

3. RESULTS AND DISCUSSION

3.1 Fragment selection

In this experiment we chose 23 various fragments (decapeptides) of metallothionein (FMT) which were selected from Expasy database. We focused on different amino acids in surrounding relatively conservative cysteine placement in each peptide. Comparison of different metallothionein proteins was performed according to the amino acid sequence of the primary structure. Similarly, there have been studied histidine residues in the sequences of metallothionein in terms of the high possibility of coordination of metal with cysteine [42]. Metallothioneins, chains with length of 60 amino acids, derived from a variety of eukaryotic organisms, which are represented by fish and mammals. The complete amino acid sequence of a total of 140 metallothioneins were first aligned by conservative sections and subsequently ten (eleven) amino acids long clusters with the highest content of cysteine were chosen. The selected clusters were also highly conservative, which was related to FMT peptide 2, which was the most conservative [35]. In addition, selected decapeptide clusters were at positions 31-40 in the initial primary sequence of metallothioneins. For some metallothioneins the length of the clusters was longer by one amino acid from ten to eleven due to alignment according to conservative amino acid sequence. Thus we were able to choose from all the available sequences that differed at least or just in one amino acid. In this way, 23 unique fragments were selected from 140 tested ones [35].

3.2 Cognition dendrogram

Selected fragments of metallothionein (FMT) were then subjected to further comparative analysis in terms of their mutual relation. Phylogenetic tree (dendrogram) showing the graphical hierarchy of the sequences is shown in Fig. 1. More detailed bioinformatic evaluation of MT amino acid composition will be published elsewhere.

Firstly, the mutual distances between all pairs of sequences were calculated as number of found mutations $\boldsymbol{n_p}$ between the two aligned sequences divided by the total number $\boldsymbol{n}$ of amino acids in the sequence (gaps were neglected). The resulting distance $\boldsymbol{p}$ is known as the proportional distance [43].However, the proportional distance does not accurately describe the evolutionary distance between two sequences. This is mainly due to the fact that the reconstructed mutation at individual positions may not correspond to the actual number of mutations, or we do not know if the given position changed several times. This difference significantly affects the result in the long period of evolutionary time and therefore greater distance values of p ($p > 0.3$), which correspond binomics probability distribution, needs to be recalculated to the Poisson distribution (Equation 1).

Equation 1: $$d = -\ln(1-p)$$

The distribution should be weighted by the number of "character" in the sequence (the number of amino acids) to obtain better similarity assessment. Weighting factor B describes the probability that one amino acid can be changed to any of the other from 20, thus B = 19/20. We modify the previous equation according to the Jukes-Cantor model. (Equation 2).

Equation 2: $$d_{JC} = -B \cdot \ln\left[1-\frac{p}{B}\right]$$

These obtained pairwise distances form distance matrix, where row and column headers consist of all sequences and matrix elements are their corresponding distances.

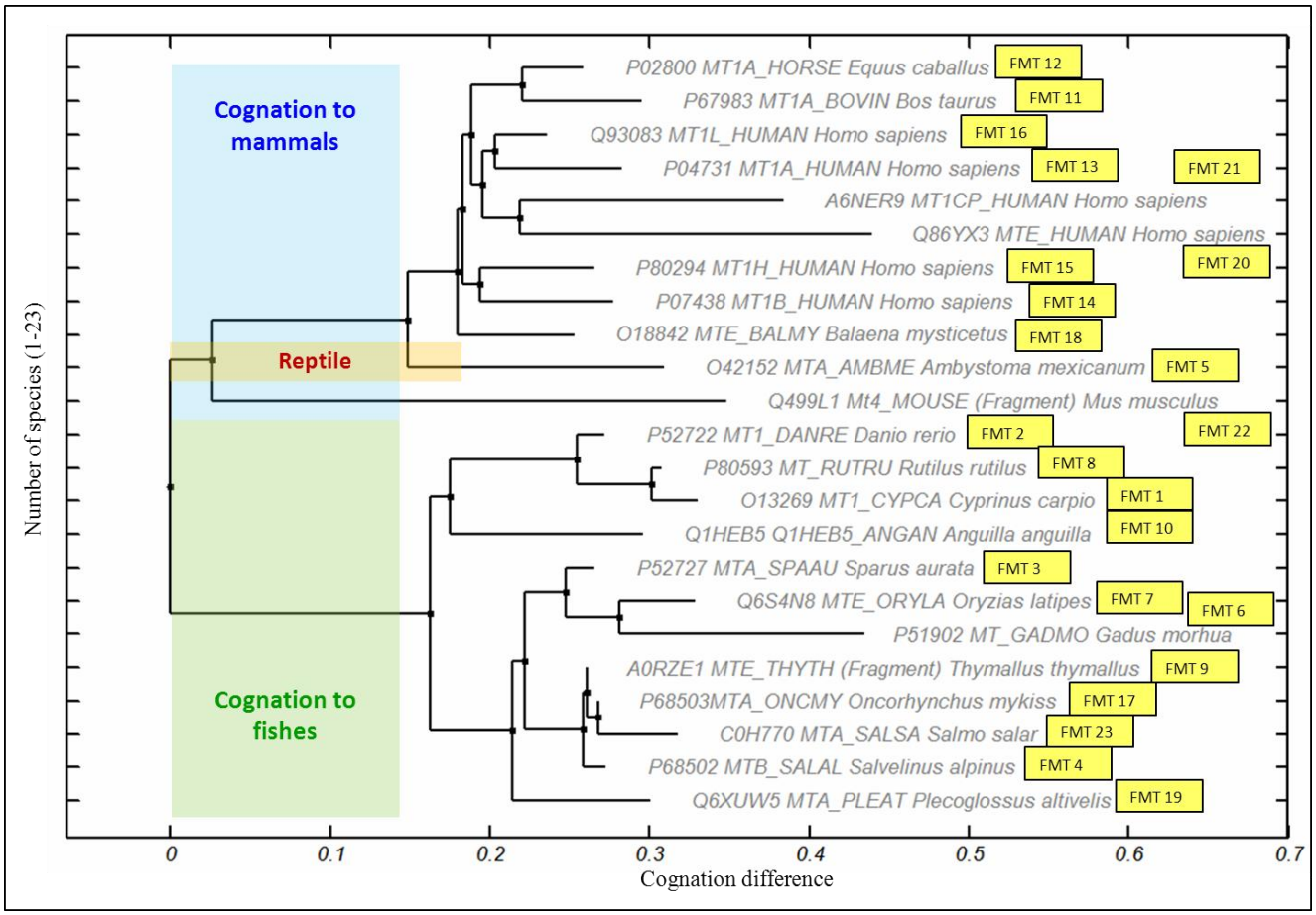

Figure 1. Cognation dendrogam for 23 selected fragments of metallothioneins according to section 3.1. Based on the analysis of data, three groups were found: a) mammals; b) reptile and c) fishes.

Secondly, BIONJ model was used [36], for searching two closest sequences at each step according to minimum evolution rules of "nearest neighbours". These sequences were selected by the

smallest mutual distance and also by their evolutionarily advantageous connection to the rest of the tree structure. This is possible due to the fact that this model calculates permutations and combinations of possible connections and selects the best one. The selected two sequences are then combined into a single node. We repeat this procedure as long as the last two connectable branches remain. The obtained dendrogram divided sequences into two basic groups of mammals and fishes (Fig. 1). It is interesting that metallothionein from the of amphibian Mexican axolotl (*Ambistoma mexicanum*) is more related to mammals than fourth isoform of metallothionein from *Mus musculus*

3.3 Hydrodynamic voltammogram measurement

After selection of the appropriate fragments, we attempted to analyze FMTs using flow injection analysis coupled with electrochemical detection (FIA-ED) and to determine hydrodynamic voltammograms (HDV) for the fragments.

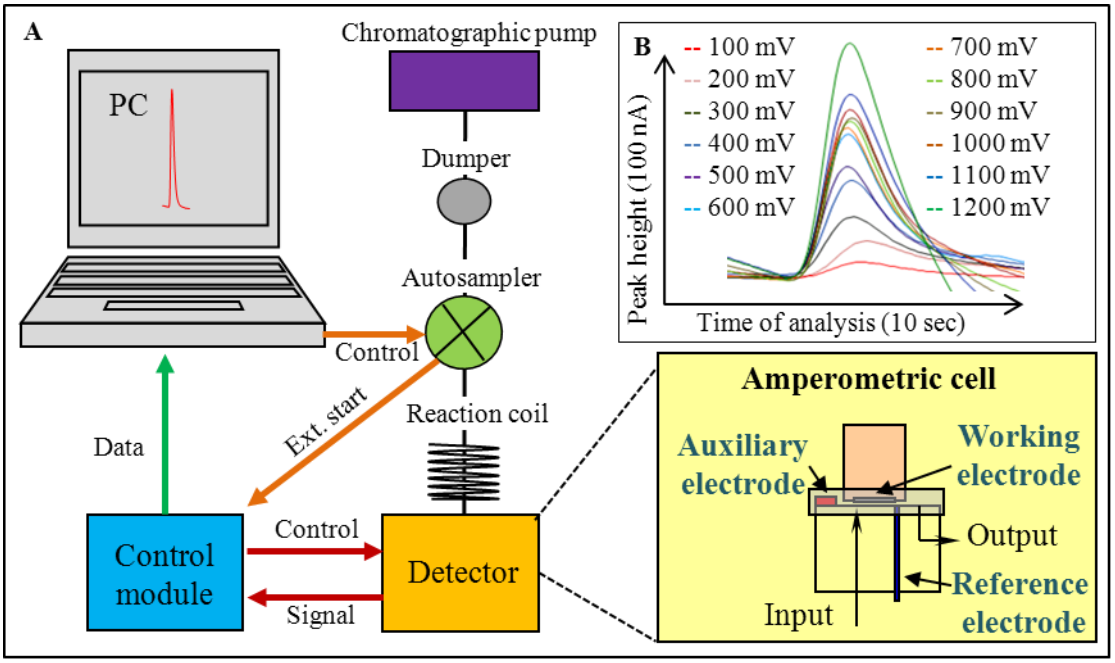

Figure 2. (**A**) Scheme of FIA – amperometric detection instrument (piston pump, dumper, autosampler, glassy carbon electrode, potentiostat and computer); in inset: arrangement of amperometric detection cell. (**B**) Hydrodynamic voltammograms of metallothionein fragment FMT-21 (100 μM, 1 $ml.min^{-1}$) as overlay of typical records from hydrodynamic voltammograms' determination.

For measuring a lot of electroanalytical data, we developed an automated system employing flow injection analysis with amperometric detection on glassy carbon electrode (electrochemical cell has 50 μl volume). For the accurate HDV determination, it had to be carried out a measurement at selected potential (100, 200, 300, 400, 500, 600, 700, 800, 900, 1000, 1100 or 1200 mV) after each injection (n = 3). Therefore potential change, which was conducted on the amperometric cell, was

driven by TIMELINE program method integrated in software of Coulochem III module (Fig. 2A). The TIMELINE cycle contained the stepwise changes of potentials in precisely defined times synchronized with times of injections of autosampler. Each cycle was started using external signal from autosampler. Autosampler was driven by Clarity software. Each cycle we obtained one full HDV profile (Fig. 2B). This setup was designed especially for our high throughput analysis needs. After each series of the HDV measurement the electrochemical cell was cleaned by changing of potential cycles twice from -1200 to +1200 mV. Each cycle was taken for 30 seconds.

3.4 Optimization of the electrochemical analysis of FMTs

In order to use this method for studying the interactions of FMTs with platinum based cytostatics, we had to find the most suitable conditions for the electrochemical analysis. Primarily, the composition of mobile phase as Britton-Robinson buffer, acetate buffer and phosphate buffer, in which a detected electrochemical signal was measured at a working potential of 500 mV (based on our previously published papers [37,44]), was optimized. To obtain optimum electrochemical responses depending on pH peptides characterizing each group FMT 13 (mammal, *Homo sapiens*), FMT 5 (reptile, *Ambystoma mexicanum*) and FMT 2 (fish, *Danio rerio*) were studied in the presence of 0.04 M Britton-Robinson, 0.02 M acetate buffer and 0.05 M phosphate buffer with emphasis on neutral pH to mimic physiological environment (Fig. 3). Britton-Robinson buffer was tested within the pH range from 2 to 7. There was observed decreasing trend in current responses from pH 2 to pH 5 (down for 40 % of the maximum response). Further increase in pH to 7 resulted in a slight increase in the current response, but this increase was not sufficient for sensitive analysis of metallothionein fragments (Fig. 3A). Changes in the electrochemical behaviour of the studied fragments probably relate with the protonation of functional groups. MT protein isoelectric point (pI) is 8 under normal conditions, and we observed the great effect of this value on the electrochemical signal [45-47]. Differences between the various fragments were statistically insignificant and varied between 5 to 10%. A probable effect of the composition of the mobile phase on FMT current response is well evident for other electrolytes (acetate, phosphate). In the acetate buffer there was also decreasing trend of the current response with the increasing pH from 3 (100% of the maximum value), 4 (60% of maximum value) to 5 (10% of the maximum value, Fig. 3B). pH of phosphate buffer was tested from 5 to 8 (Fig. 3C). It clearly follows from the results obtained that electrochemical responses of the tested fragments increased with the increasing pH. Phosphate buffer pH 8 exhibits the best electrochemical signal for the tested fragments of metallothionein. The obtained results suggest significant structural changes in the tested fragments MT in the presence of various electrolytes with various pH. pH 5 (independently of the composition of the environment) would likely lead to a peptide folding structure and thus there could be worse interaction with glassy carbon electrode surface.

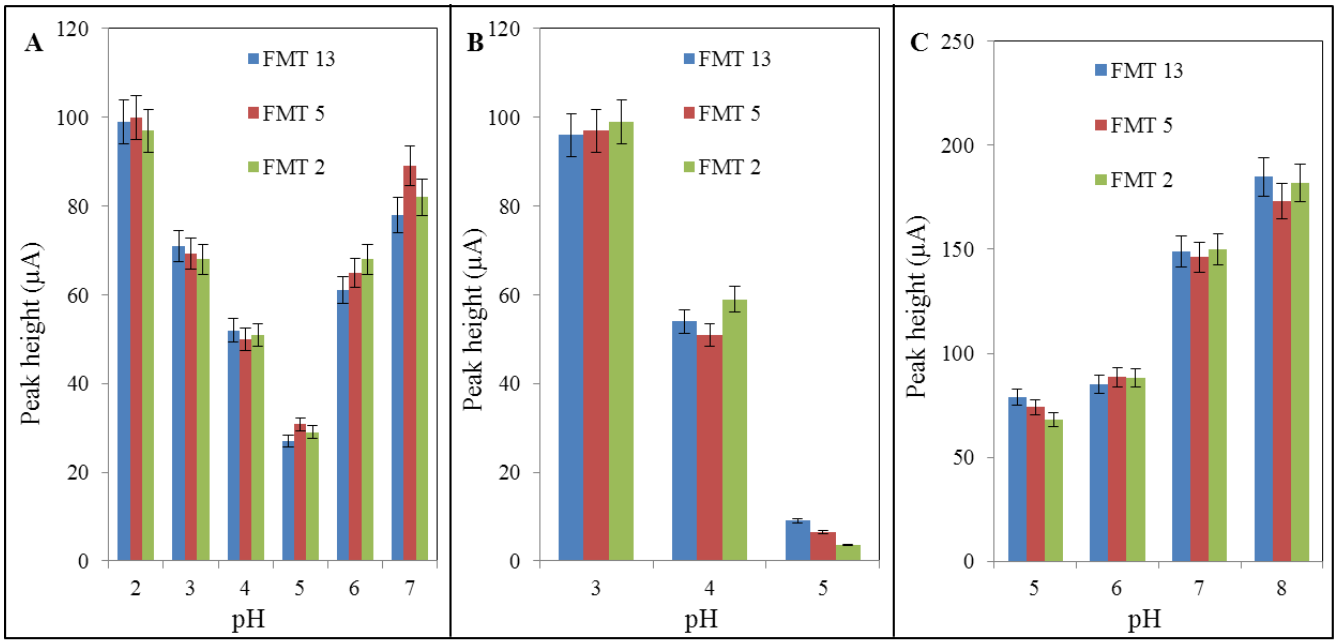

Figure 3. Influence of the pH range of selected buffers on current responses of FMTs 2, 5 and 13. (**A**) 0.04 M Britton Robinson buffer (pH 2 – 7). (**B**) 0.02 M acetate buffer (pH 3 – 5). (**C**) 0.05 M phosphate buffer (pH 5 – 8). FMT 13 (mammal, *Homo sapiens*), FMT 5 (reptile, *Ambystoma mexicanum*) and FMT 2 (fish, *Danio rerio*) at 1 µg.ml^{-1}, flow rate: 1 ml.min-1, applied potential: 500 mV, glassy carbon electrode, cell volume 50 µl, injection: 10 µl, n = 3.

Electrochemical detection is dependent on the presence of the electroactive substance at the electrode surface (interphase electrode-solution). Electrode processes describes Nernst-Peters equation (balance between electrode and ions activity at the surface of the electrode, Equation 3). The rate control step is the diffusion overvoltage, which is proportional to the concentration of analyte.

Equation 3: $$\eta D = (RT/zF)\cdot\ln(a_1/a_o)$$

Transport of the electroactive substance at the electrode is determined by the existence of a concentration gradient dc/dx and rules according to I. Fick law in the event of a stirred solution (or moving electrode, Equation 4).

Equation 4: $$I = -zF\cdot dn/dt = zFDA\cdot(co - c1)/\delta$$

Based on Equations 3 and 4 it is clear that the electrode processes in the flow system are extremely complex and require separate experimental studies. From the electroanalytical point of view monitoring of FMTs' signal changes was carried (Fig. 4). Under a flow rate from 0.5 to 0.75 ml.min^{-1}, the signal was detected for longer time, which was reflected in the width of the recorded signal (about 30 ms). The effect of signal tailing decreased with the increase in the flow rate to the flow rate of 1 ml.min^{-1}, where the sum of the peak heights was the highest. On the contrary, increasing flow rate for 0.25 and 0.5 ml.min^{-1} caused a decrease in detected current responses. This is probably due to less

accessibility of the analyte to the surface of the working electrode, which can be attributed to the limited diffusion, which occurs with a higher flow rate of mobile phase.

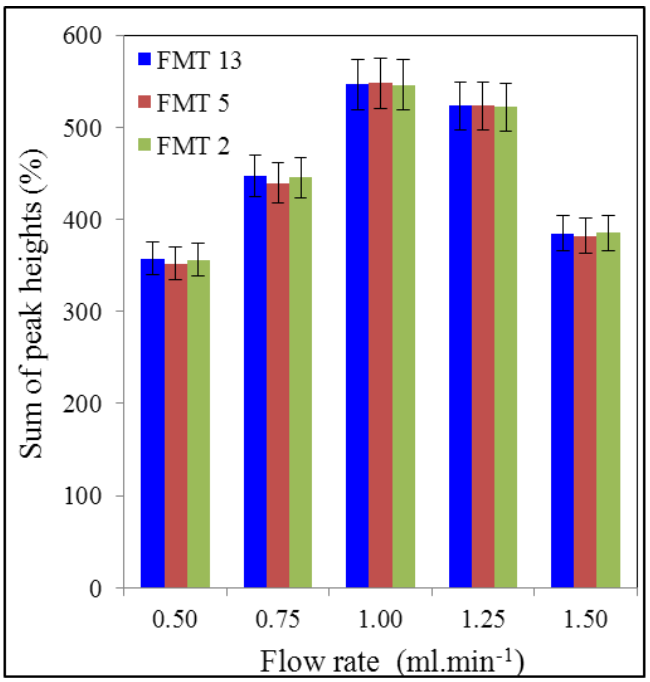

Figure 4. The influence of flow rate on amperometric response of three representative FMTs as FMT 13 (mammal, *Homo sapiens*), FMT 5 (reptile, *Ambystoma mexicanum*) and FMT 2 (fish, *Danio rerio*) at 100 μM. For other details see Fig. 3.

3.5 Electrochemical behaviour of MT fragments

After the reaching the best electrochemical conditions we analysed the samples of FMTs using FIAED. This was carried out by repetitive injections of a sample in different potentials to obtain hydrodynamic voltammogram (HDV) within the range from 100 to 1200 mV with the 100 mV potential step. Typical HDV is shown in Fig. 5A. The current response increases slowly up to reaching interval of redox important applied potential. In this interval, the increase in current responses is rapid (inflection point). After that interval, the current response does not change much. Ideally, the working electrode should be inert to the electrolytic solution and only respond to the analyte in a thermodynamically defined, potential-dependent fashion. Many times this is not the case. The kinetics of heterogeneous charge transfer between the electrode and the analyte, in addition to the reactivity of the electrode itself, enter into the situation. Electrochemical reactivity can be altered considerably by changing the electrode material. In many cases, this can be highly advantageous. The large hydrogen overpotential characteristic of mercury electrodes in protic solutions extends the attainable negative potential range (past carbon) and makes difficult reduction reactions possible. For this reason, mercury remains the material of choice in these potential regions. However, the reduction of dissolved oxygen, a very facile reaction on mercury over a wide potential range, does not occur till negative-potential

region on a glassy carbon electrode [48]. We divided the fragments of metallothionein (100 µM) according the source organism into the five groups. The number of fragments in each group was strictly dependent on the structural composition or low conservativity respectively.

3.5.1 First group

The first group includes only one fragment which comes from MT of *Ambystoma mexicanum* (K-SCCSCCPSE) which is phylogenetically the oldest one in the whole selected unit. It´s HDV has 100 – 600 mV rapid increasing trend and the plateau thus isn´t noticeable. Between potentials 550 to 1000 mV is the increase slighter. The maximum of HDV was found under applied potential 900 mV and from 1100 mV HDV was rapid increase (Fig. 5B).

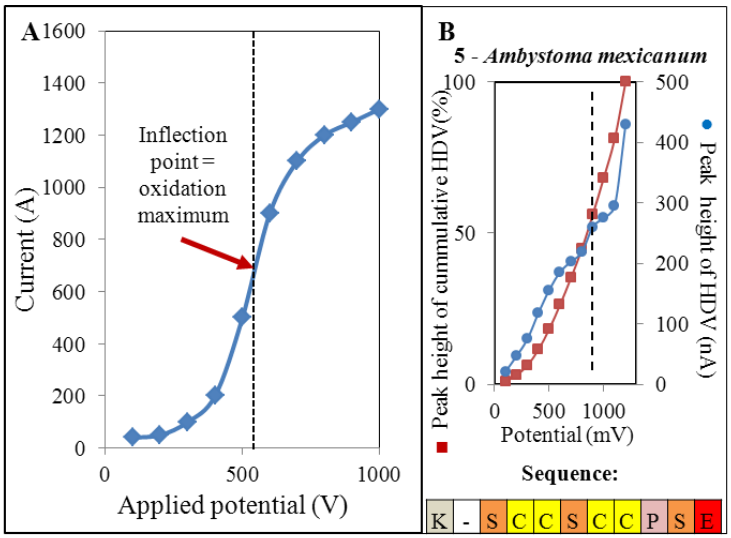

Figure 5. (**A**) Model of cumulative HDV and its maximum, which is taken as inflection point of the HDV curve. (**B**) Hydrodynamic voltammogram (100, 200, 300, 400, 500, 600, 700, 800, 900, 1000, 1100, 1200 mV) of metallothionein fragment from I. group – 5 - *Ambystoma mexicanum* and it´s amino acid sequence, n = 3. For other details see Fig. 4.

3.5.2 Second group

The next group "Freshwater fishes" contained 7 species, of which FMTs were rather different. The trend of HDV of *Cyprinus carpio* was from 100 mV to 600 mV rapidly increased and reached 200 nA as the highest response. A plateau of the HDV was found within the range from 600 to 1100 mV (current differences app. 30 nA) and the inflection point was detected at 900 mV. From 1100 mV strong increasing of HDV (current app. 400 nA) was noticed (Fig. 6A). Another species *Danio rerio* had precipitous increasing of HDV from 100 to 550 mV (current app 290 nA) followed by a plateau to 1000 mV (current differences about 20 nA) and rapid increasing trend from 1000 to 1200 mV (maximum current 490 nA). The maximum oxidation (inflection point) of MT fragment was measured at 600 mV (Fig. 6B). HDV fragment MT *Salvelinus alpinus* differed markedly. It had gradual

increasing trend of HDV from 100 to 900 mV (current app. 150 nA), where the maximum was determined. From 900 – 1000 mV (current differences app. 5 nA) the short plateau followed by a rapid increase to 1200 mV (Fig. 6C). The trend of HDV of *Oryzias latipes* had increased from 100 to the maximum of HDV 800 mV. The plateau of this HDV was very negligible (100 – 800 mV, current 280 nA) because of the HDV was increased after the maximum was achieved (Fig. 6D). From 700 – 1000 mV (current differences app. 80 nA) the short plateau followed by rapid increase of current response to 1200 mV. The course of HDV *Rutilus rutilus* (K-SCCTCCPSG) had gradual trend from 100 mV to 700 mV (current 100 nA) where the maximum was estimated. After the short plateau 800 – 950 mV (current differences app. 40 nA) rapid increasing trend of HDV to 1200 mV (maximum current about 250 nA) was detected (Fig. 6E). HDV of *Thymallus thymallus* (KPSCCDCCPSG) showed precipitous increasing from 100 mV to 600 mV (app. 400 nA), where the lowest maximum of HDV was estimated. The long plateau from 600 mV to 1000 mV (current differences app. 110 nA) was followed by the increasing of HDV to 1200 mV (maximum current about 650 nA, Fig. 6F). The last species of freshwater fishes *Anguilla anguilla* (K-SCCSCCPST) had the most rapid increasing trend of HDV from 100 mV to 400 mV (current difference app. 160 nA) followed by wide plateau ending at 1000 mV (current differences app. 30 nA). The inflection point was found at 900 mV (Fig. 6G). Average inflection point of this group was 771 mV with the highest maximum inflection point of the HDV at 900 mV and the lowest maximum at 600 mV. Changes in amino acids composition in the chain and at the end mainly influence the HDV behaviour of studied FMTs (Fig. 6).

3.5.3 Third group

Group of saltwater fishes contained 5 species. The trend of HDV of *Sparus aurata* (K-SCCSCCPAG) was increasing from 100 mV to 500 mV (current app. 200 nA) followed by a plateau (from 500 to 1000 mV, current differences app. 70 nA), which was ending at 1000 mV. Under the potential range from 1000 to 1200 mV a rapid increase in HDV was found (current 500 nA, Fig. 7A). HDV of *Gadus morhua* (K-SCCECCPSG) showed increasing trend from 100 to 650 mV (current app. 380 nA) with a plateau from 700 to 900 mV (current differences app. 20 nA) followed by a gradual increase to 1200 mV (maximum current about 580 nA). The inflection point was detected at 700 mV (Fig. 7B). Another fish *Oncorhynchus mykiss* (KASCCDCCPSG) had gradual increasing trend of HDV from 100 to 550 mV (current app. 190 nA), where the inflection point 600 mV was estimated. The plateau of 600 – 700 mV (current differences app. 5 nA) of this HDV wasn´t significant but followed by noticeable increasing trend to 1200 mV and current maximum at 510 nA (Fig. 7C). HDV of *Plecoglossus altivelis* (KTSCCSCCPAG) shows short increasing trend from 100 mV to 500 mV (current response app. 120 nA) and an HDV long plateau from 500 to 900 mV (current differences app. 70 nA) with the inflection point at 900 mV. From 900 to 1200 mV there was observed rapid increasing trend of the current response with the highest response of 510 nA (Fig. 7D). *Salmo salar* (KASCWDCCPSG) had the strong increasing trend of HDV with a fractional plateau. This fragment is of the highly different primary structure, which is the reason for various electrochemical behaviours. Amperometric signal was increasing rapidly up to 750 mV with current maximum at 290 nA (Fig. 7E).

An HDV plateau from 750 to 1050 mV (current differences app. 100 nA) with the inflection point of 1050 mV was detected. Average maximum of a group of saltwater fishes was 840 mV with the highest maximum as 1000 mV and the lowest maximum as 600 mV.

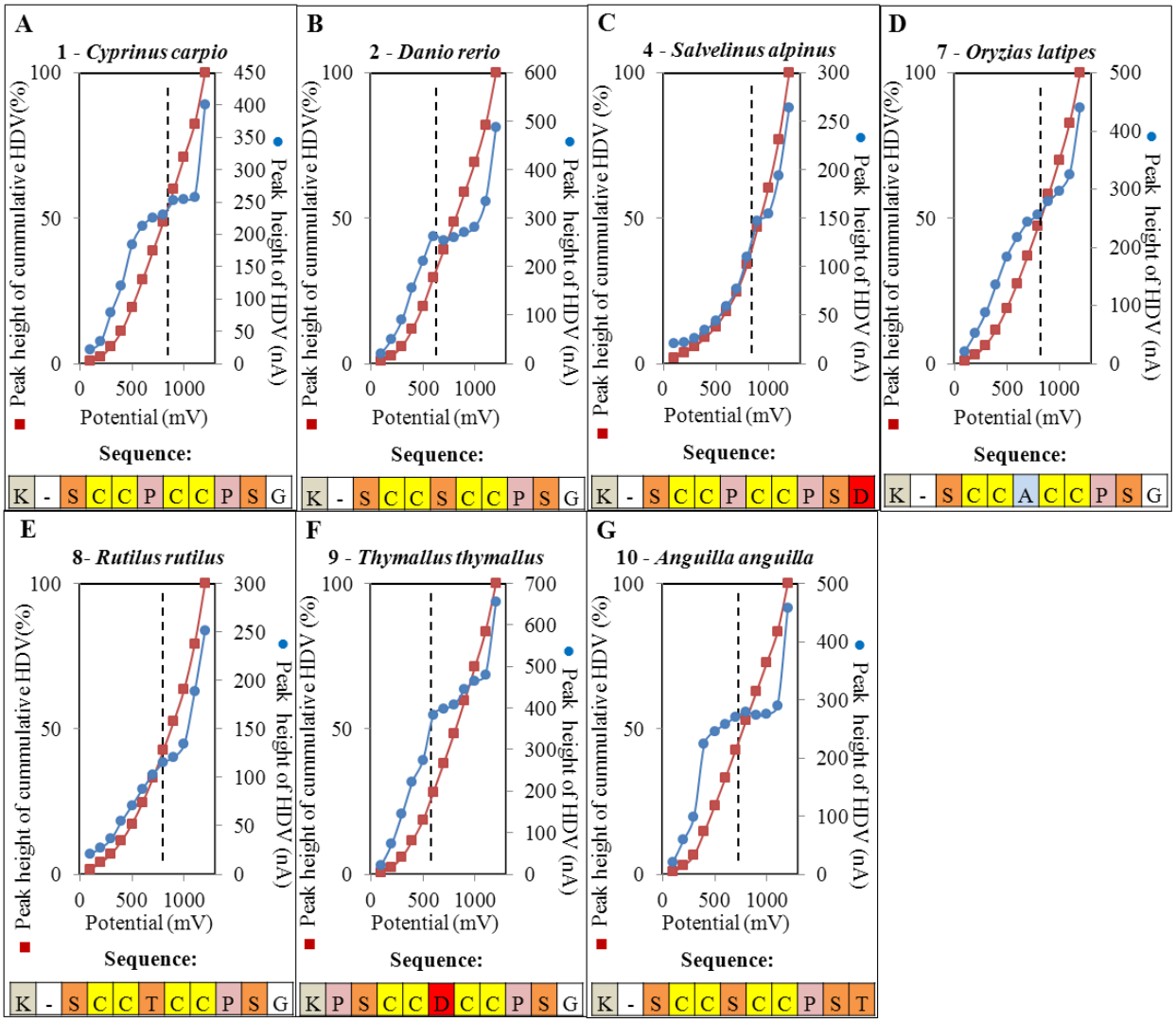

Figure 6. Hydrodynamic voltammograms of Metallothionein fragments from II. group - freshwater fishes (**A**) 1 – *Cyprinus carpio*. (**B**) 2 – *Danio renio*. (**C**) 4 – *Salvelinus alpinus*. (**D**) 7 – *Orvizas latipes*. (**E**) 8 – *Rutilus rutilus*. (**F**) 9 – *Thvmallus thymallus*. (**G**) 10 – *Anguilla anuilla* and their amino acid sequences. For other details see Fig. 5.

3.5.4 Fourth group

Forth group contained 4 species of mammals. HDV of *Bos taurus* (K-SCCSCCPVG) had increasing trend from 100 – 500 mV (current response app. 200 nA) and the plateau was from 600 to 1000 mV (current differences app. 110 nA). The inflection point of HDV was determined at 600 mV (Fig. 8A). HDV of *Equus caballus* (K-SCCSCCPGG) showed a graduate increase from 100 to 450 mV (current response app. 270 nA). The long plateau was measured from 500 to 1000 mV (current

differences app. 80 nA) with the inflection point of 800 mV and it was followed by a very rapid increase (maximum current response app. 600 nA, Fig. 8B). *Balaena mysticetus* (K-SCCSCCPPG) had increasing trend of HDV from 100 to 600 mV (current response about 350 nA, Fig. 8C). HDV of this fragment showed the plateau from 600 to 900 mV followed by a graduate increase in current response with applied potential. The inflection point was determined at 700 mV (current differences app. 10 nA). The last species of this category *Mus musculus* (K-SCCPCCPPG) had rapid trend of HDV in the interval from 100 to 500 mV. The plateau determined between 700 and 1100 mV (current response app. 50 nA) was long and ended by the sharp increase in current (maximum current app. 470 nA). The inflection point of HDV was obtained at 700 mV (Fig. 8D). Average maximum of HDV in IV. group was 700 mV with the highest maximum at 800 mV and the lowest maximum at 600 mV. It clearly follows from the obtained results that ending amino acids, the presence of GG or PP in the cysteine cluster had the most considerable effect on HDVs (Fig. 8).

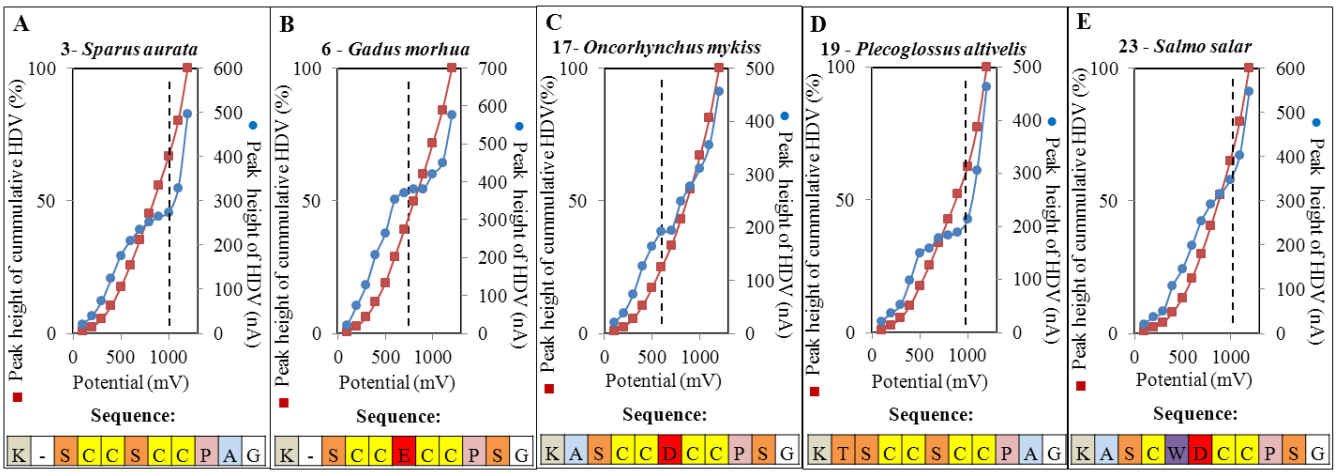

Figure 7. Hydrodynamic voltammograms of Metallothionein fragments from III. group – saltwater fishes (**A**) 3 – *Sparus aurata*. (**B**) 6 – *Gadus morhua*. (**C**) 17 – *Oncorhynchus mykiss*. (**D**) 19 – *Plecoglossus altivelis*. (**E**) 23 – *Salmo salar* and their amino acid sequences. For other details see Fig. 5.

3.5.5 Fifth group

The final group of *Homo sapiens* contained 6 various subtype fragments of metallothionein. It is a heterogeneous group from the point of the primary structure, which is well documented by the obtained HDVs. MT1A_HUMAN (K-SCCSCCPMS) showed increased trend of HDV within the range from 100 to 450 mV and the long plateau within the interval from 500 to 1100 mV (current differences app. 50 nA) with the inflection point at 900 mV (Fig. 9A). The HDV of MT1B_HUMAN (K-CCCSCCPVG) increased within the interval from 100 to 600 mV (current response app. 250 nA). The HDV plateau was estimated from 600 to 800 mV with the inflection point at 600 mV.

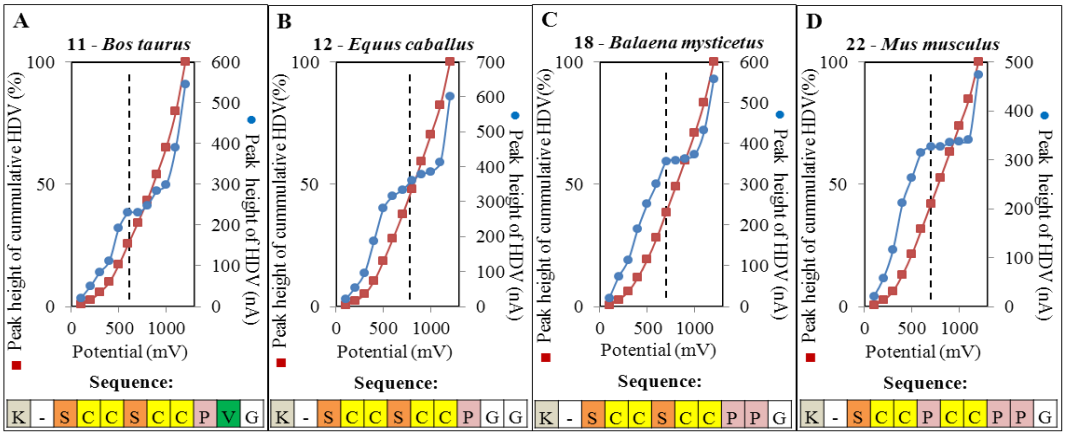

Figure 8. Hydrodynamic voltammograms of metallothionein fragments from IV. group - mammals (**A**) 11 – *Boss taurus*. (**B**) 12 – *Eauus caballus*. (**C**) 18 – *Balaena mysticetus*. (**D**) 22 – *Mus musculus* and their amino acid sequences. For other details see Fig. 5.

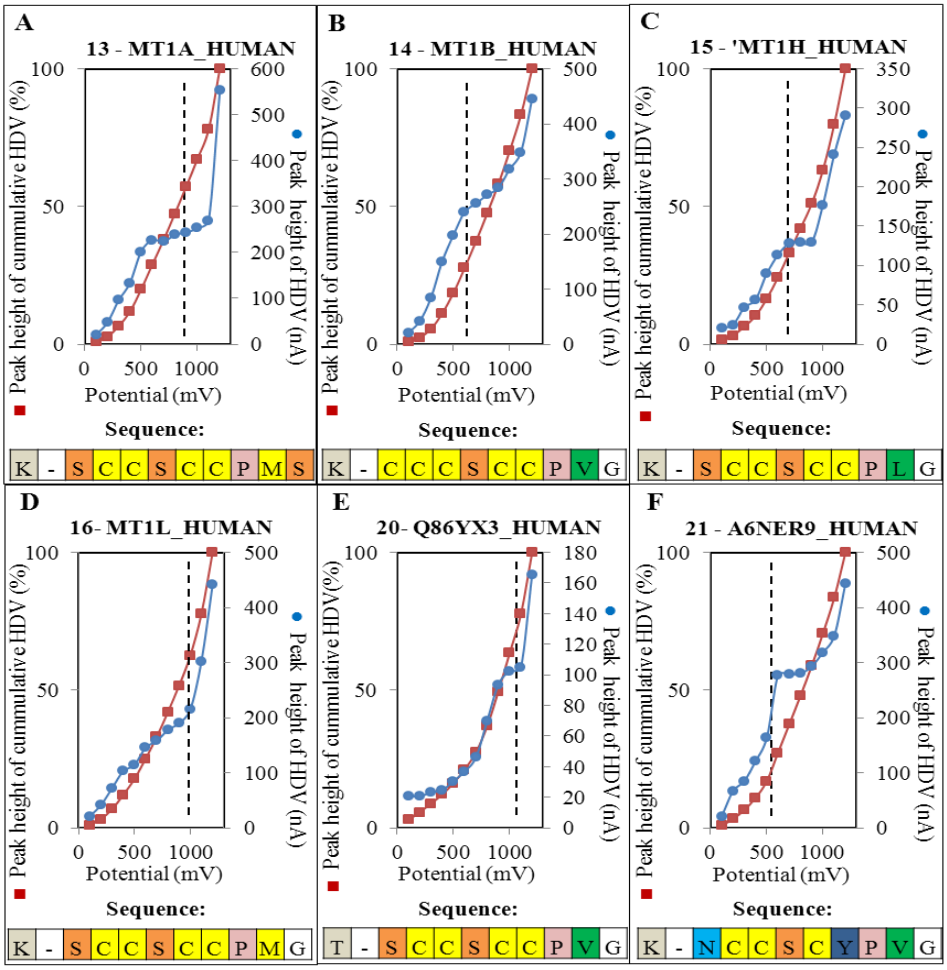

Figure 9. Hydrodynamic voltammograms of Metallothionein fragments from V. group – Homo sapiens (**A**) 13 – MT1A_HUMAN. (**B**) 14 - MT1B_HUMAN. (**C**) 15 – MT1H_HUMAN. (**D**) 16 – MT1L_HUMAN. (**E**) 20 – Q86YX3_HUMA. (**F**) 21 – A6NER9_HUMAN and their amino acid sequences. For other details see Fig. 5.

From 800 to 1200 mV there was measured the increasing trend (maximum current response was app. 460 nA, Fig. 9B). MT1H_HUMAN (K-SCCSCCPLG) had increasing prolonged trend of HDV within the interval from 100 to 700 mV followed by a plateau from 700 to 850 mV (current differences app. 10 nA) with the inflection point at 700 mV and increasing trend from 900 to 1200 mV (maximum current response app. 290 nA, Fig. 9C). The fragment of metallothionein of MT1L_HUMAN (K-SCCSCCPMG) showed increasing trend within the interval from 100 to 550 mV and the long plateau from 600 to 1000 mV (current differences app. 100 nA). The inflection point at 1000 mV was followed by the increasing trend of HDV to 1200 mV with maximum current response app. 430 nA (Fig. 9D). Q86YX3_HUMAN (T-SCCSCCPVG) had gradually increasing trend of HDV from 100 to 850 mV with the short plateau from 1000 to 1100 mV (current differences app. 40 nA). The inflection point was detected at 1000 mV (Fig. 9E). The last one A6NER9_HUMAN (K-NCCSCYPVG) showed intensive increasing trend within the interval from 100 to 500 mV. MT HDV plateau (from 500 to 800 mV; current differences app 30 nA) and the inflection point at 600 mV followed by gradually increasing of HDV to 1200 mV (maximum current app. 440 nA) was measured (Fig. 9F). The average maximum of HDV was at 800 mV with the highest maximum at 1000 mV and the lowest maximum at 600 mV. This group of fragments has various HDVs. Changes in K for T in the very first position in the primary structure caused dramatic changes in the electrochemical behaviour. In addition, changes in cysteine cluster had the considerable effect on the behaviour.

3.6 Comparison of HDVs

It clearly follows from the results obtained that FMTs could be divided into the specific groups not only according to their electrochemical behaviour but also according to their primary structure. For the final interpretation we compared oxidation maxima obtained for each tested group. We were interested how the oxidation maxima were influenced in the case of different groups. With regards to the findings which were published elsewhere [49] the oxidation maxima of the peptide was increasing with the higher amount of thiol groups, which were preferably for binding metals. Based on these facts we can assume on the suitability of the FMT to be more attractive to the metal while it has higher oxidation maxima. Total count of the oxidation maximum determined from HDVs within an individual group was averaged and is shown in Fig. 10. With regards to differences in the values obtained it can be concluded that *Ambystoma mexicanum* had a highest value. Freshwater fishes had slightly lower average HDV maxima as compared with maxima of the saltwater fishes. A group of "*Homo sapiens*" had a higher oxidation maximum than other "mammals". The current maximum is characterized as a sum of peak height (nA) in applied potential of groups. We found that the mammals had the highest current maximum. An average value for all species in the group of mammals was 317 nA. *Ambystoma mexicanum* had the current maximum at 260 nA, freshwater fishes at 244 nA, saltwater fishes at 278 and homo sapiens at 200 nA. Further we compared the average plateau wide of the tested groups. As we demonstrated above, some species didn´t have the plateau, especially *Ambystoma mexicanum*, *Oryzias latipes*, MT1L_HUMAN and *Mus musculus*. Their HDV showed precipitous trend. The freshwater fishes (273 mV) and mammals (275 mV) had the widest plateaus (Fig. 10). Other groups

had the plateau wide as 216 mV for *Homo sapiens* and 200 mV for saltwater fishes. The changes determined by three abovementioned parameters for observed groups are resulting from differences in the amino acid composition of the studied fragments.

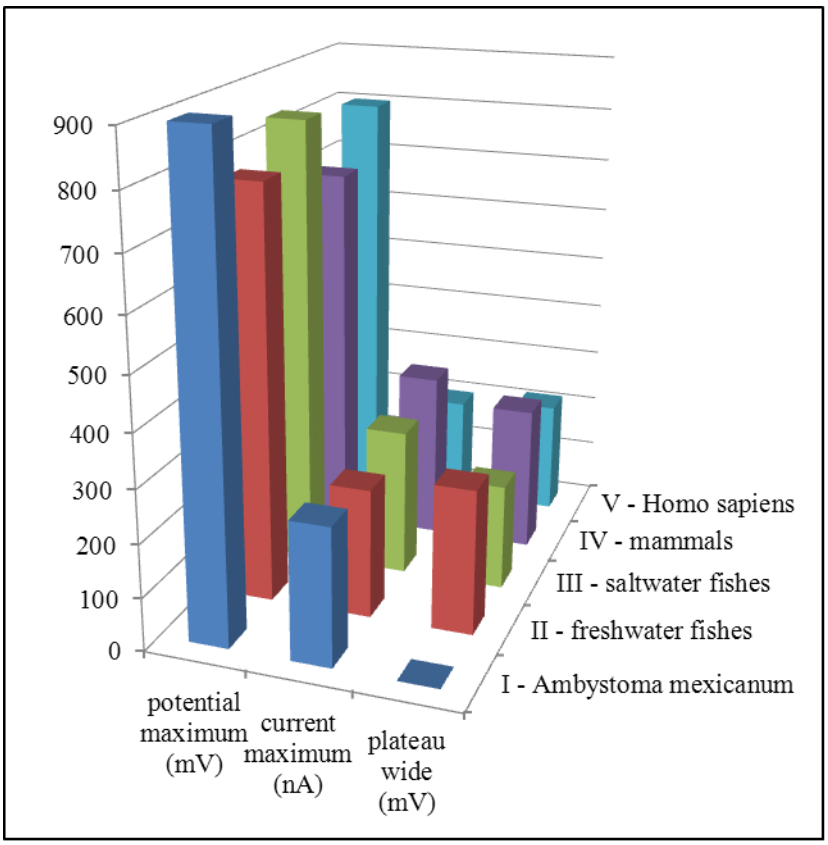

Figure 10. Maxima of the oxidation potentials obtained from hydrodynamic voltammograms of metallothionein fragments of I. – V. groups. For other details see Fig. 5.

4. CONCLUSIONS

Due to high frequency of cysteine occurrence in the primary structure of metallothionein it is possible to determine a sequence, which contributes to the metal binding. For the study of the interaction with metals it is suitable to choose a special sequence (peptide) of metallothionein and, then to study it by suitable methods [50]. In our study we determined the 23 metallothionein fragments, which were based on the primary structure of these proteins in various organisms to find differences in their electrochemical behaviour. The differences were found and could be related to their affinity to metal ions.

ACKNOWLEDGEMENTS
This work has been supported by IGA MENDELU IGA IP23/2012, NANOSEMED GA AV KAN208130801, CEITEC CZ.1.05/1.1.00/02.0068 and by the project for conceptual development of research organization 00064203.

References

1. M. Margoshes and B. L. Vallee, *J. Am. Chem. Soc.*, 79 (1957) 4813.
2. V. Adam, I. Fabrik, T. Eckschlager, M. Stiborova, L. Trnkova and R. Kizek, *TRAC-Trends Anal. Chem.*, 29 (2010) 409.
3. T. Eckschlager, V. Adam, J. Hrabeta, K. Figova and R. Kizek, *Curr. Protein Pept. Sci.*, 10 (2009) 360.
4. V. Supalkova, D. Huska, V. Diopan, P. Hanustiak, O. Zitka, K. Stejskal, J. Baloun, J. Pikula, L. Havel, J. Zehnalek, V. Adam, L. Trnkova, M. Beklova and R. Kizek, *Sensors*, 7 (2007) 932.
5. R. Dallinger, B. Berger, P. Hunziker and J. H. R. Kagi, *Nature*, 388 (1997) 237.
6. B. Gold, H. Deng, R. Bryk, D. Vargas, D. Eliezer, J. Roberts, X. Jiang and C. Nathan, *Nat. Chem. Biol.*, 4 (2008) 609.
7. J. Kagi, T. L. Coombs, J. Overnell and M. Webb, *Nature*, 292 (1981) 495.
8. E. J. Kelly and R. D. Palmiter, *Nature Genet.*, 13 (1996) 219.
9. N. J. Robinson, *Nat. Chem. Biol.*, 4 (2008) 582.
10. M. Valls, S. Atrian, V. de Lorenzo and L. A. Fernandez, *Nat. Biotechnol.*, 18 (2000) 661.
11. M. Sato and I. Bremner, *Free Radic. Biol. Med.*, 14 (1993) 325.
12. K. Nakazato, K. Nakajima, T. Kusakabe, K. Suzuki and T. Nagamine, *Pathol. Int.*, 58 (2008) 765.
13. A. T. Miles, G. M. Hawksworth, J. H. Beattie and V. Rodilla, *Crit. Rev. Biochem. Mol. Biol.*, 35 (2000) 35.
14. B. A. Masters, C. J. Quaife, J. C. Erickson, E. J. Kelly, G. J. Froelick, B. P. Zambrowicz, R. L. Brinster and R. D. Palmiter, *J. Neurosci.*, 14 (1994) 5844.
15. P. Trayhurn, J. S. Duncan, A. M. Wood and J. H. Beattie, *Am. J. Physiol.-Regul. Integr. Comp. Physiol.*, 279 (2000) R2329.
16. C. O. Simpkins, *Cell. Mol. Biol.*, 46 (2000) 465.
17. O. Zitka, M. Ryvolova, J. Hubalek, T. Eckschlager, V. Adam and R. Kizek, *Curr. Drug Metab.*, 13 (2012) 306.
18. P. Coyle, J. C. Philcox, L. C. Carey and A. M. Rofe, *Cell. Mol. Life Sci.*, 59 (2002) 627.
19. S. G. Bell and B. L. Vallee, *ChemBioChem*, 10 (2009) 55.
20. M. Ryvolova, S. Krizkova, V. Adam, M. Beklova, L. Trnkova, J. Hubalek and R. Kizek, *Curr. Anal. Chem.*, 7 (2011) 243.
21. D. Hynek, S. Krizkova, L. Krejcova, J. Gumulec, M. Ryvolova, N. Cernei, M. Masarik, V. Adam, L. Trnkova, M. Stiborova, T. Eckschlager, J. Hubalek and R. Kizek, *Int. J. Electrochem. Sci.*, 7 (2012) 1749.
22. D. Hynek, J. Prasek, J. Pikula, V. Adam, P. Hajkova, L. Krejcova, L. Trnkova, J. Sochor, M. Pohanka, J. Hubalek, M. Beklova, R. Vrba and R. Kizek, *Int. J. Electrochem. Sci.*, 6 (2011) 5980.
23. L. Krejcova, I. Fabrik, D. Hynek, S. Krizkova, J. Gumulec, M. Ryvolova, V. Adam, P. Babula, L. Trnkova, M. Stiborova, J. Hubalek, M. Masarik, H. Binkova, T. Eckschlager and R. Kizek, *Int. J. Electrochem. Sci.*, 7 (2012) 1767.
24. S. Krizkova, M. Ryvolova, J. Gumulec, M. Masarik, V. Adam, P. Majzlik, J. Hubalek, I. Provaznik and R. Kizek, *Electrophoresis*, 32 (2011) 1952.
25. S. Krizkova, M. Ryvolova, D. Hynek, T. Eckschlager, P. Hodek, M. Masarik, V. Adam and R. Kizek, *Electrophoresis*, 33 (2012) 1824.
26. M. Masarik, J. Gumulec, M. Sztalmachova, M. Hlavna, P. Babula, S. Krizkova, M. Ryvolova, M. Jurajda, J. Sochor, V. Adam and R. Kizek, *Electrophoresis*, 32 (2011) 3576.
27. M. Ryvolova, D. Hynek, H. Skutkova, V. Adam, I. Provaznik and R. Kizek, *Electrophoresis*, 33 (2012) 270.
28. J. Sochor, D. Hynek, L. Krejcova, I. Fabrik, S. Krizkova, J. Gumulec, V. Adam, P. Babula, L. Trnkova, M. Stiborova, J. Hubalek, M. Masarik, H. Binkova, T. Eckschlager and R. Kizek, *Int. J. Electrochem. Sci.*, 7 (2012) 2136.

29. J. Mendieta, J. Chivot, A. Munoz and A. R. Rodriquez, *Electroanalysis*, 7 (1995) 663.
30. A. Munoz and A. R. Rodriguez, *Electroanalysis*, 7 (1995) 674.
31. I. Sestakova and P. Mader, *Cell. Mol. Life Sci.*, 46 (2000) 257.
32. O. Nieto and A. R. Rodriguez, *Bioelectrochem. Bioenerg.*, 40 (1996) 215.
33. C. Harlyk, G. Bordin, O. Nieto and A. R. Rodriguez, *Electroanalysis*, 9 (1997) 608.
34. N. M. Marshall, D. K. Garner, T. D. Wilson, Y. G. Gao, H. Robinson, M. J. Nilges and Y. Lu, *Nature*, 462 (2009) 113.
35. O. Zitka, H. Skutkova, V. Adam, L. Trnkova, P. Babula, J. Hubalek, I. Provaznik and R. Kizek, *Electroanalysis*, 23 (2011) 1556.
36. O. Gascuel, *Mol. Biol. Evol.*, 14 (1997) 685.
37. O. Zitka, M. A. Merlos, V. Adam, N. Ferrol, M. Pohanka, J. Hubalek, J. Zehnalek, L. Trnkova and R. Kizek, *J. Hazard. Mater.*, 203 (2012) 257.
38. O. Zitka, H. Skutkova, O. Krystofova, P. Sobrova, V. Adam, J. Zehnalek, L. Havel, M. Beklova, J. Hubalek, I. Provaznik and R. Kizek, *Int. J. Electrochem. Sci.*, 6 (2011) 1367.
39. P. Babula, D. Huska, P. Hanustiak, J. Baloun, S. Krizkova, V. Adam, J. Hubalek, L. Havel, M. Zemlicka, A. Horna, M. Beklova and R. Kizek, *Sensors*, 6 (2006) 1466.
40. S. Krizkova, O. Krystofova, L. Trnkova, J. Hubalek, V. Adam, M. Beklova, A. Horna, L. Havel and R. Kizek, *Sensors*, 9 (2009) 6934.
41. R. Mikelova, J. Baloun, J. Petrlova, V. Adam, L. Havel, H. Petrek, A. Horna and R. Kizek, *Bioelectrochemistry*, 70 (2007) 508.
42. C. A. Blindauer, M. T. Razi, D. J. Campopiano and P. J. Sadler, *J. Biol. Inorg. Chem.*, 12 (2007) 393.
43. K. Tamura, M. Nei and S. Kumar, *Proc. Natl. Acad. Sci. U. S. A.*, 101 (2004) 11030.
44. D. Potesil, J. Petrlova, V. Adam, J. Vacek, B. Klejdus, J. Zehnalek, L. Trnkova, L. Havel and R. Kizek, *J. Chromatogr. A*, 1084 (2005) 134.
45. R. Kizek, J. Vacek, L. Trnkova, B. Klejdus and L. Havel, *Chem. Listy*, 98 (2004) 166.
46. R. Prusa, R. Kizek, L. Trnkova, J. Vacek and J. Zehnalek, *Clin. Chem.*, 50 (2004) A28.
47. L. Trnkova, R. Kizek and J. Vacek, *Bioelectrochemistry*, 56 (2002) 57.
48. K. Aoki, K. Tokuda and H. Matsuda, *J. Electroanal. Chem.*, 209 (1986) 247.
49. O. Zitka, M. Kominkova, S. Skalickova, H. Skutkova, I. Provaznik, T. Eckschlager, M. Stiborova, L. Trnkova, V. Adam and R. Kizek, *Sci Rep*, submitted (2012).
50. P. Kotrba, L. Doleckova, M. Pavlik and T. Ruml, *Biotechnol. Tech.*, 10 (1996) 773.